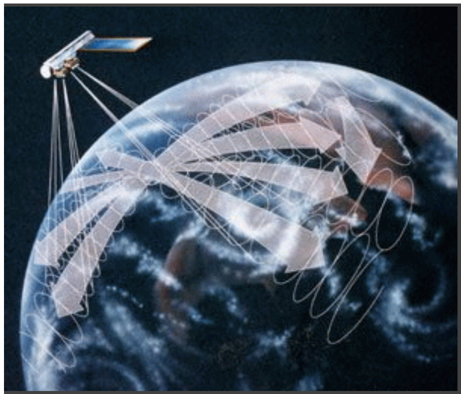

CERES Angular Distribution Model Working Group Report

Wenying Su
Wenying.Su-1@nasa.gov
NASA LaRC, Hampton VA

Lusheng Liang   Zachary Eitzen   Sergio Sejas
SSAI, Hampton VA

  

From radiance to flux: angular distribution models

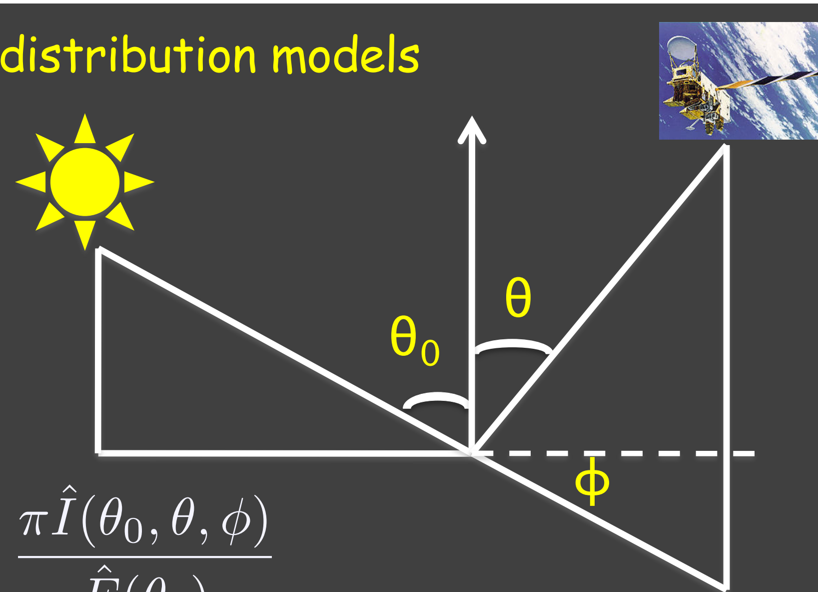

- Sort observed radiances into angular bins over different <u>scene types</u>;
- Integrate radiance over all θ and ϕ to estimate the anisotropic factor for each scene type:

$$R(\theta_0, \theta, \phi) = \frac{\pi \hat{I}(\theta_0, \theta, \phi)}{\int_0^{2\pi} \int_0^{\frac{\pi}{2}} \hat{I}(\theta_0, \theta, \phi) cos\theta sin\theta d\theta d\phi} = \frac{\pi \hat{I}(\theta_0, \theta, \phi)}{\hat{F}(\theta_0)}$$

- For each radiance measurement, first determine the <u>scene type</u>, then apply scene type dependent anisotropic factor to observed radiance to derive TOA flux:

$$F(\theta_0) = \frac{\pi I_o(\theta_0, \theta, \phi)}{R(\theta_0, \theta, \phi)}$$

Outline

- CERES instrument on NPP is in full biaxial scan.
- Validation of the microwave-based and imager-based sea ice fraction against the in-situ measurements.
- SW unfiltering algorithm update.
- Inter-comparison of collocated Terra and Aqua CERES over the polar regions.

NPP RAP sample distribution: 202004

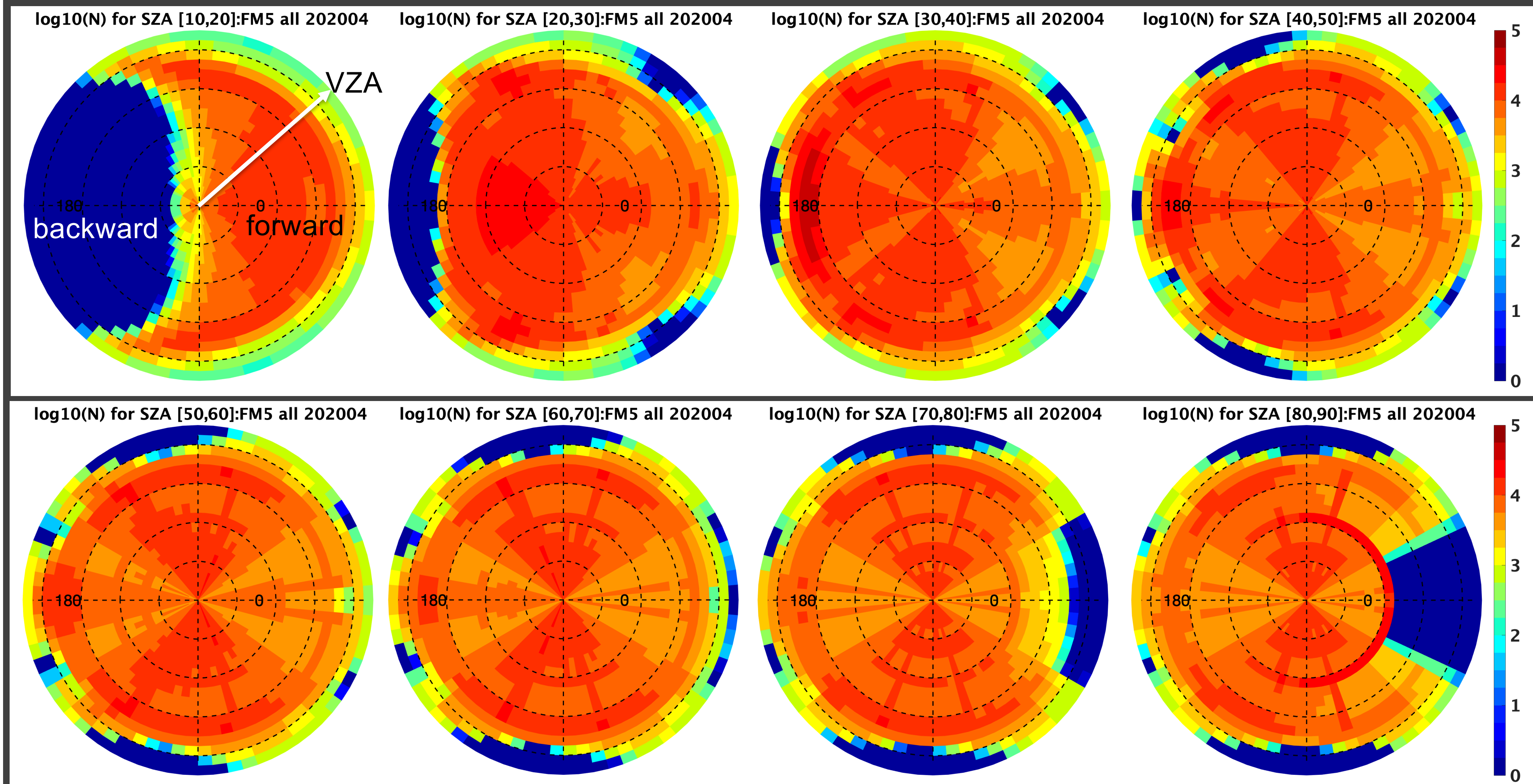

Aqua RAP scan sample distribution: 200404

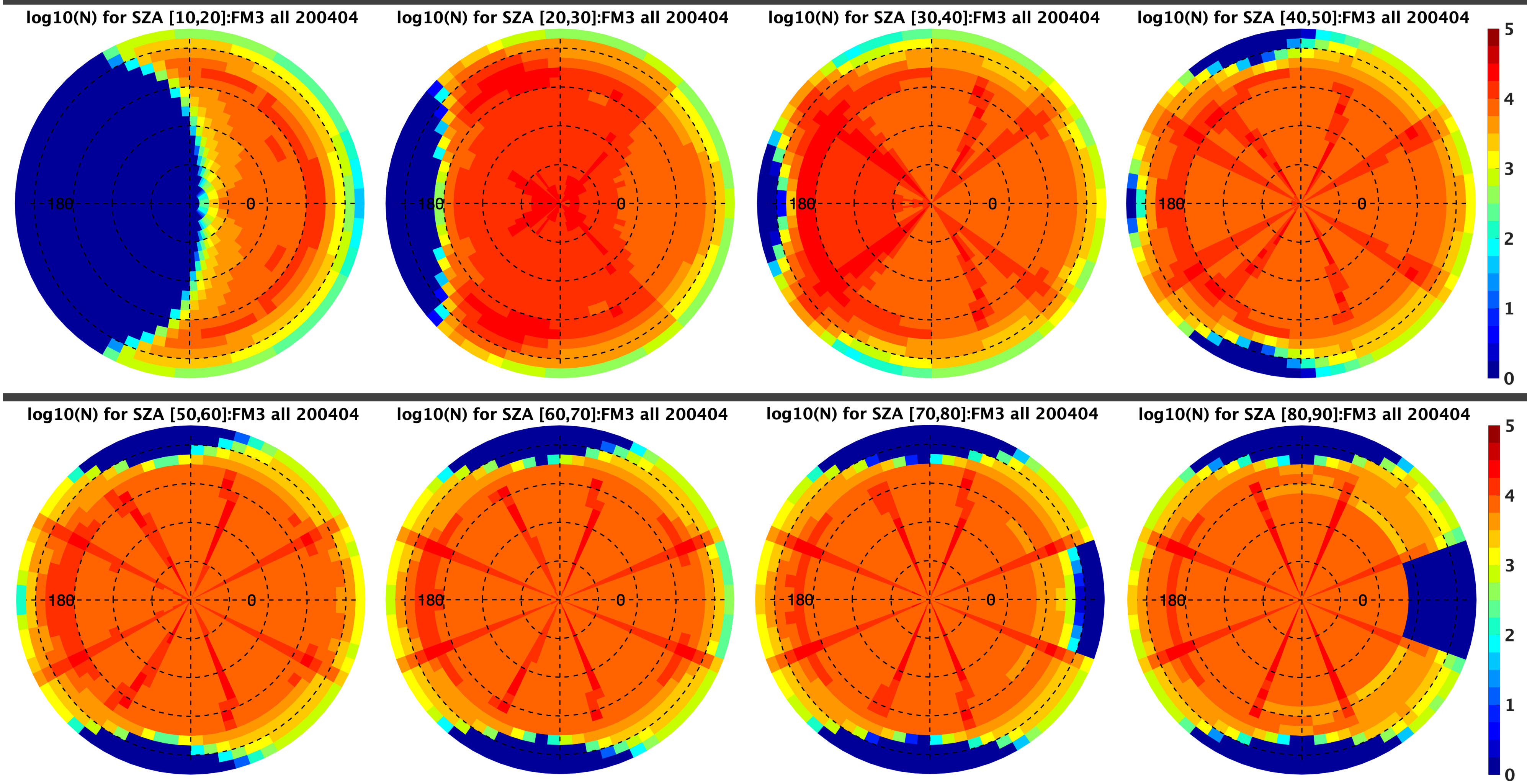

CERES NPP has more observation for near-overhead sun conditions

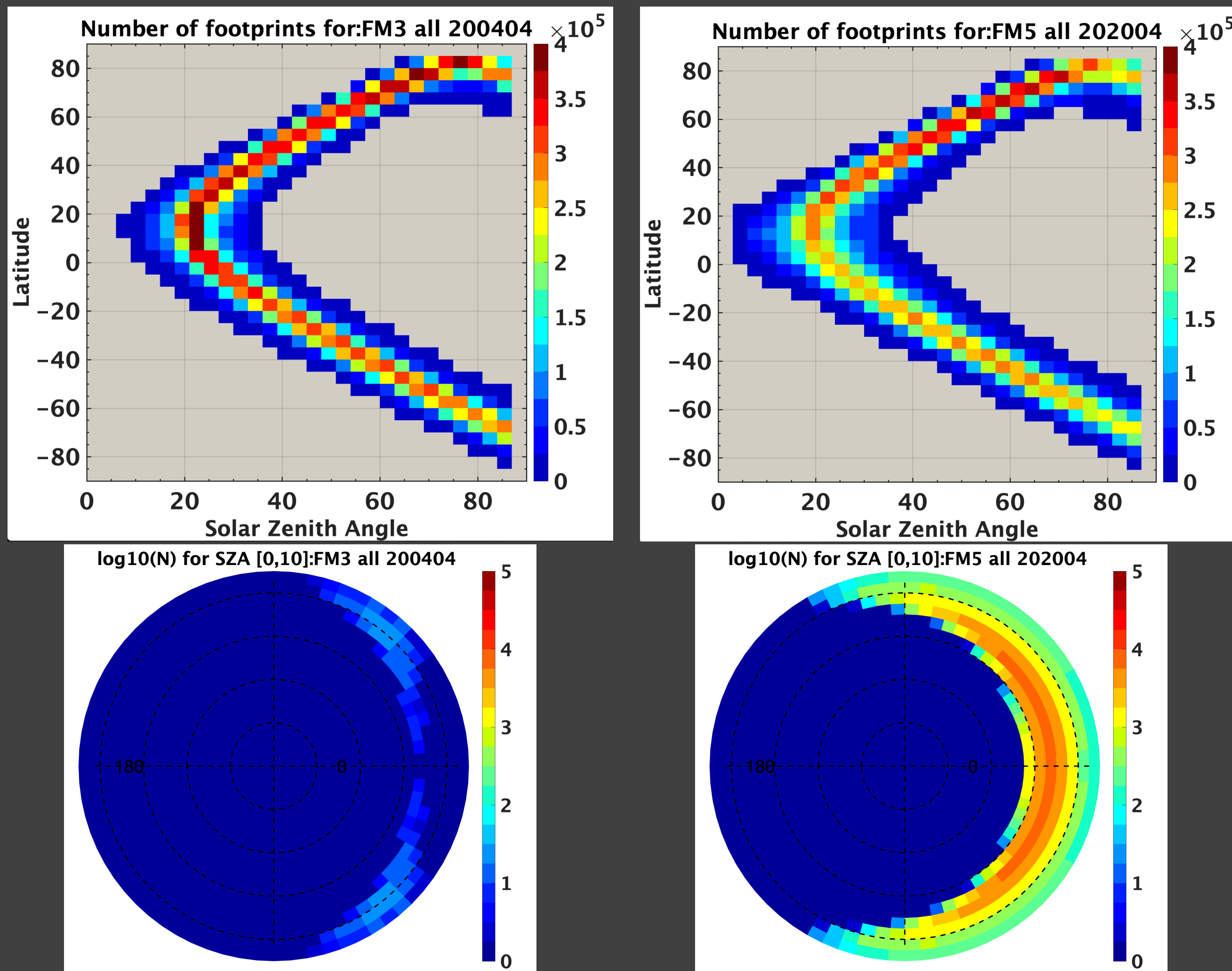

Snow and ice information in the CERES SSF data: microwave-based

- Microwave-based snow/ice fraction from NSIDC/NESDIS
  - The NSIDC (National Snow and Ice Data Center) snow/ice map is from the Near-Real-Time SSM/I-SSMIS EASE-Grid Daily Global Ice Concentration and Snow Extent product (Near-real-time Ice and Snow Extent, NISE).
  - NISE provides daily, global near-real-time maps of sea ice concentrations and snow extent using passive microwave data from the Special Sensor Microwave Imager/Sounder (SSMIS) on board the Defense Meteorological Satellite Program (DMSP) F17 satellite.
  - Sea ice concentration is determined using the NASA Team Algorithm (NTA).
  - Snow presence is determined using a modified version of the algorithm from *Chang et al.* (1987) and is detailed in *Armstrong and Brodzik* (2001).
  - NESDIS snow/ice map is also produced using microwave data. It is only used when NSIDC data is not available.

Snow and ice information in the CERES SSF data: Imager-based from cloud mask algorithm

- Snow/ice tests only apply to clear MODIS pixels
- Daytime non-polar cloud mask
  - Snow tests over land excludes land area within 30°S-25°N with elevation < 1000m.
  - Snow detection was unintentionally applied to coastal regions due to changes in microwave snow/ice default value.
  - Snow detection vary in different branches. In general, the combinations of Ref2.1/Ref0.6, T3.7-T11, IR, T11, Tskin, and microwave snow map were used.
- Daytime polar mask
  - Basic tests rely on Ref2.1, Ref3.7, and T3.7-T11
  - Additional tests: Ref2.1/Ref0.6, T11, Ref0.6, Tskin, Ref1.38, T11-T12
  - Super Cold Plateau (Antarctica and Greenland) have separate tests mainly using T6.7-T11, T11-T13.3
- Nighttime and twilight mask:
  - T37-T11, T11-T12, IR, T11, Tskin, T67-T11, T11-T13.3, microwave snow/ice maps etc are used.

From Qing Trepte

NSIDC and imager-based snow ice fraction differ

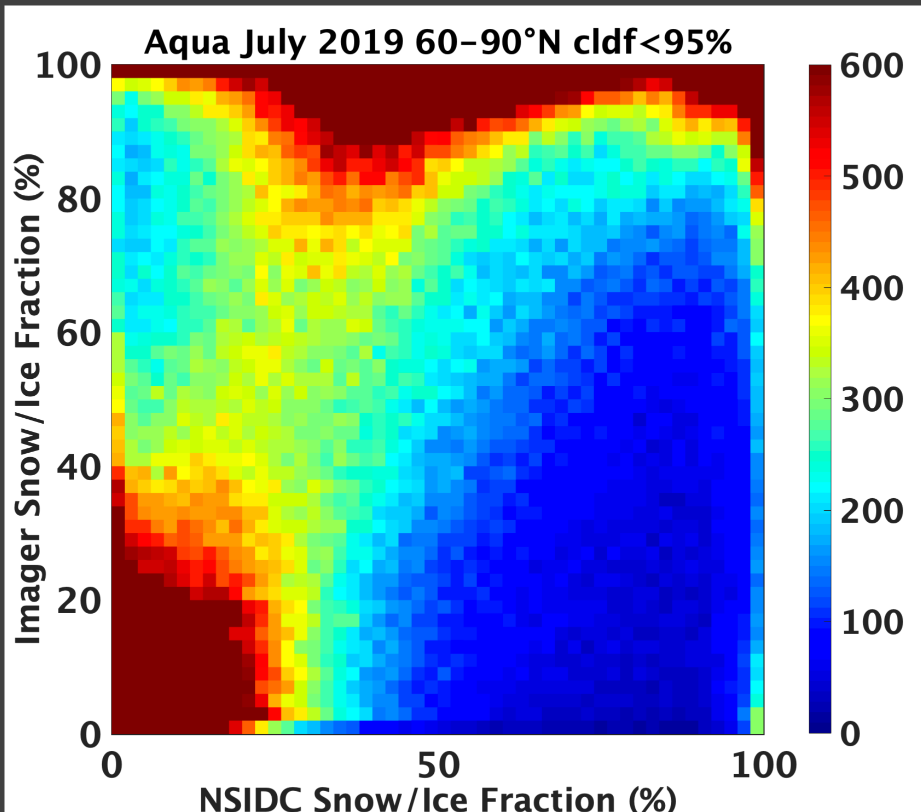

NSIDC mean=67.3%
Imager mean =84.5%
RMSE=30.6%

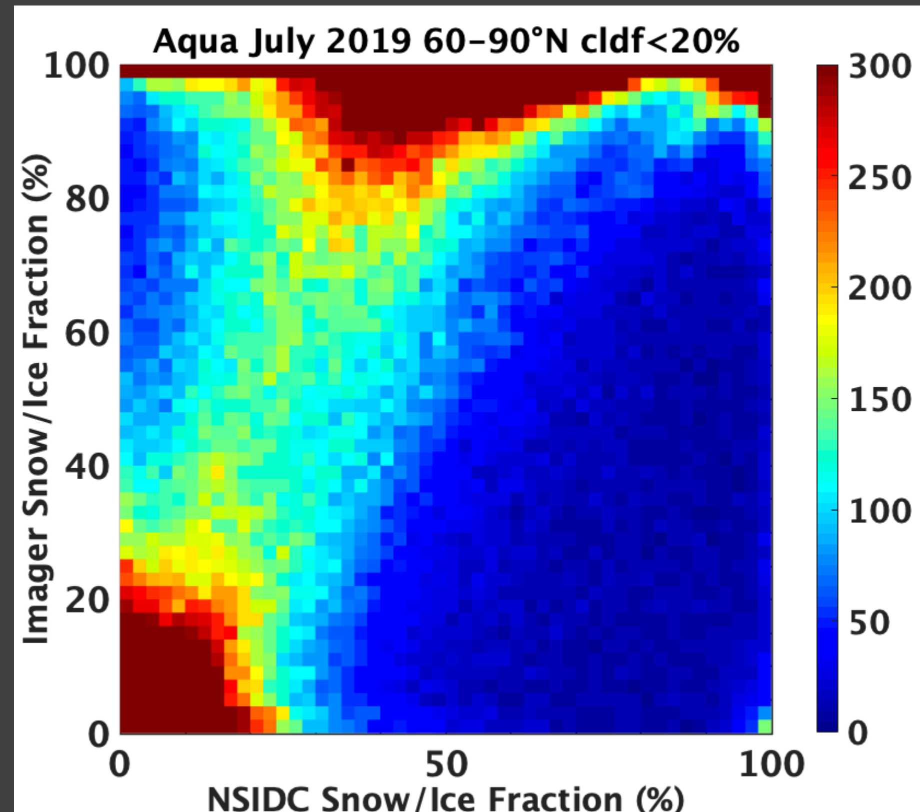

NSIDC mean=73.2%
Imager mean =87.3%
RMSE=25.4%

Number of footprints within each 1° by 1° that have snow/ice fraction >0 when both GMAO and imager-based surface skin temperature >280 K

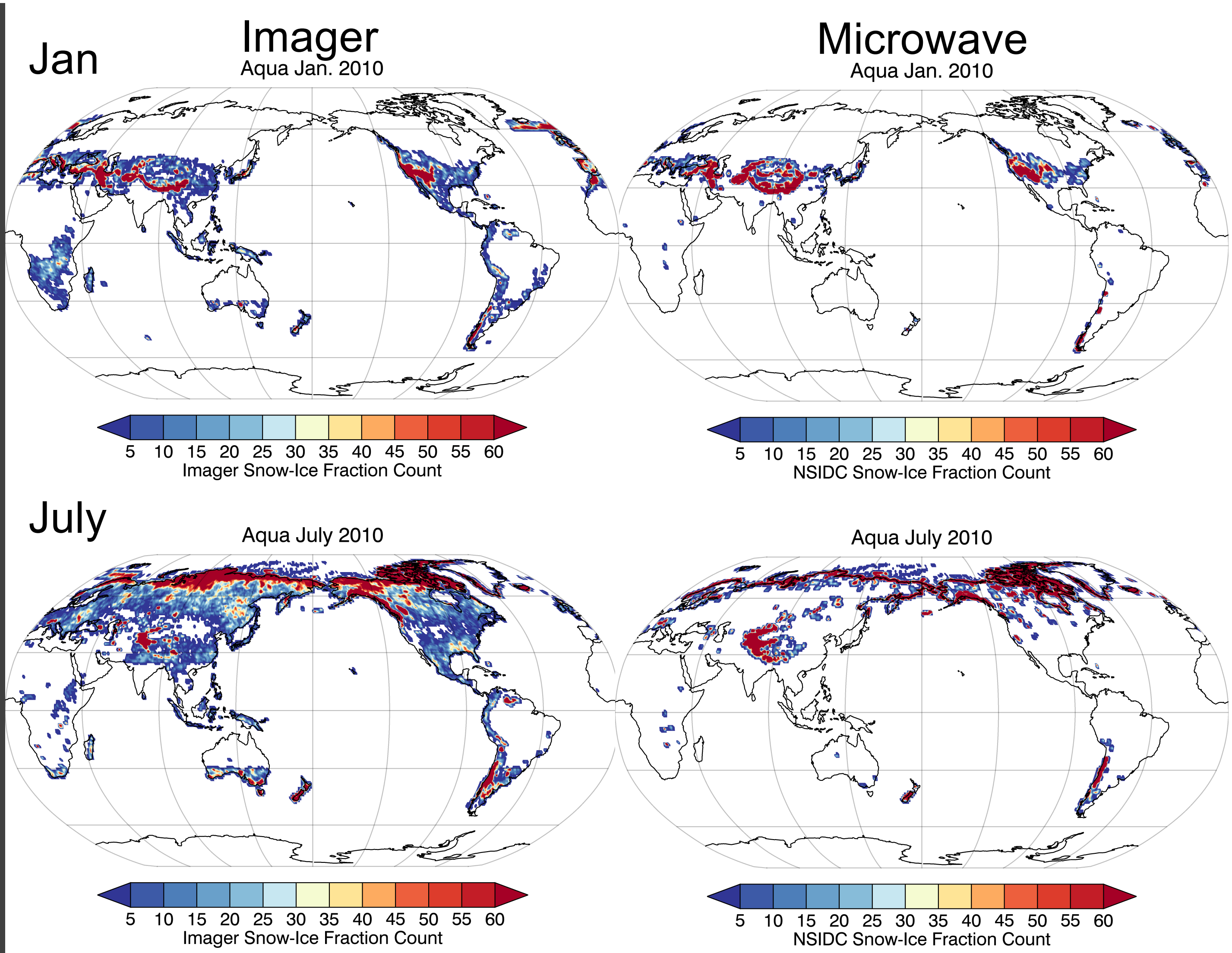

In-situ sea ice observations from Polarstern

- Scientists onboard Polarstern routinely observe the sea ice conditions around the ice breaker from the bridge by visual surveillance
- Sea ice concentration from eight cruises are used here to validate the imager-based and the microwave-based sea ice concentration in the SSF data

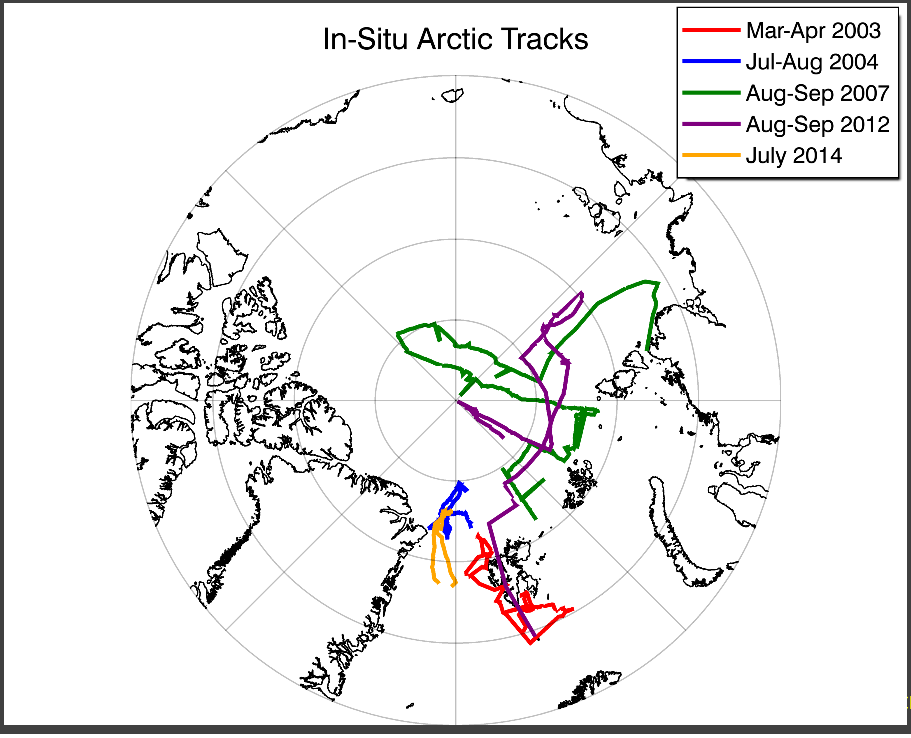

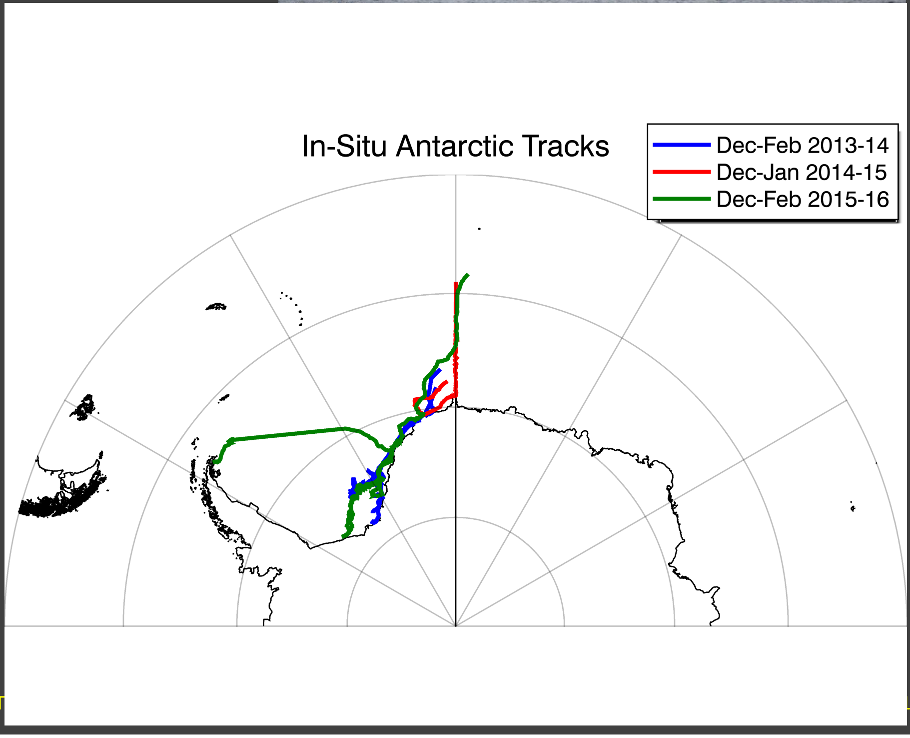

Sea ice fraction comparison between SSF and in-situ observations: all-sky

- Match SSF footprints with in-situ observations
  - Time difference < 1 hour
  - Distance difference < 10 km

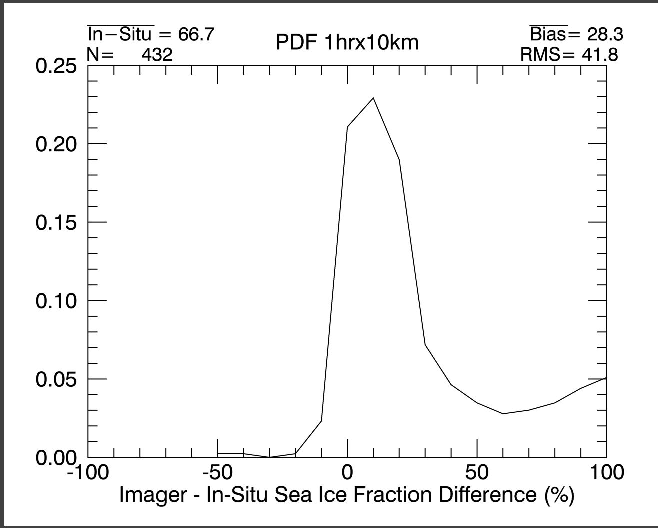

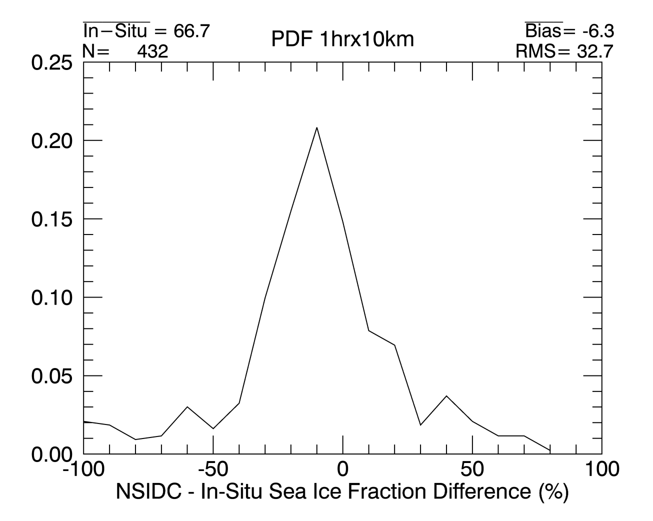

- Sea ice fraction does not vary much within a day;
- Match SSF footprints with in-situ observations
  - Time difference < 12 hour
  - Distance difference < 10 km

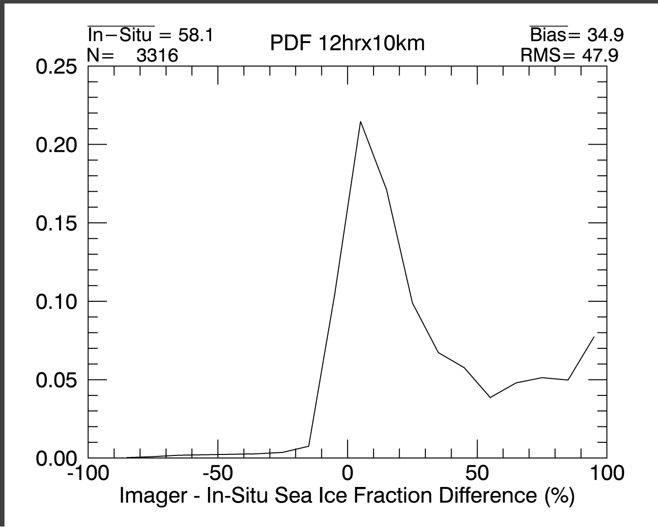

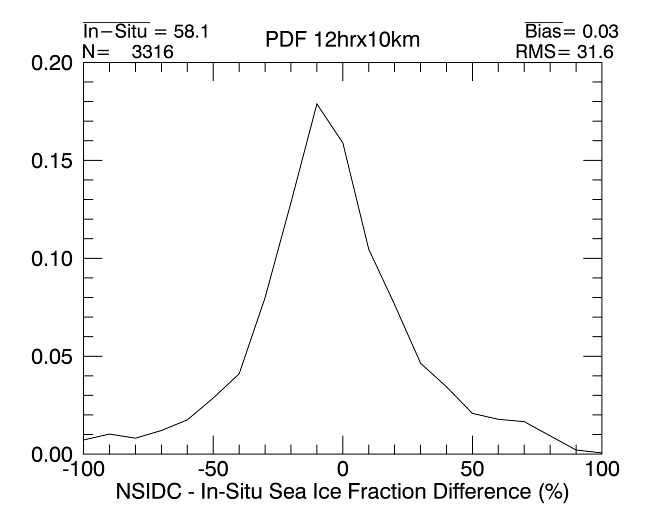

Sea ice fraction comparison between SSF and in-situ observations: NH vs SH

- Imager-based sea ice fraction is greater than in-situ observation by 25% over NH, and by 50% over SH.
- Microwave-based sea ice fraction is smaller than in-situ observation by 9% over NH, but greater than in-situ observation by 14% over SH.

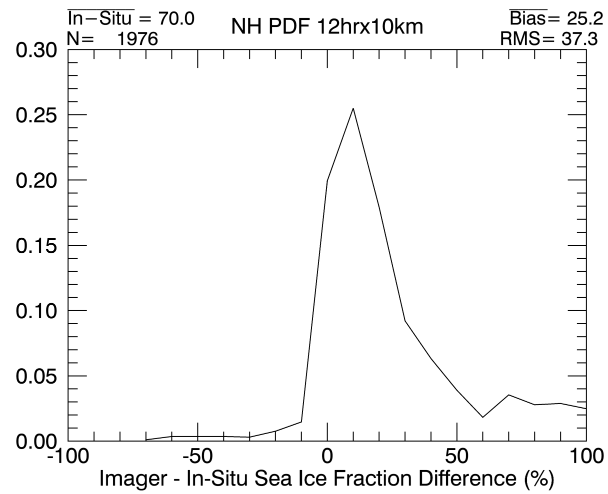

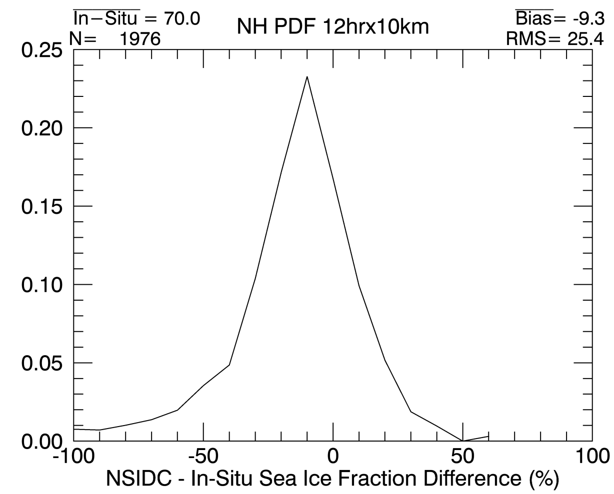

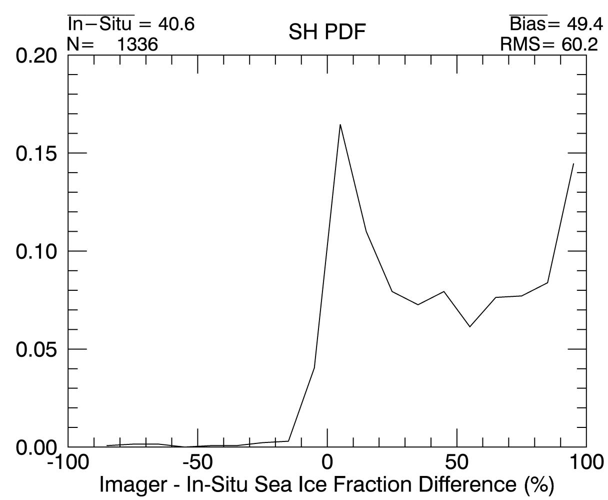

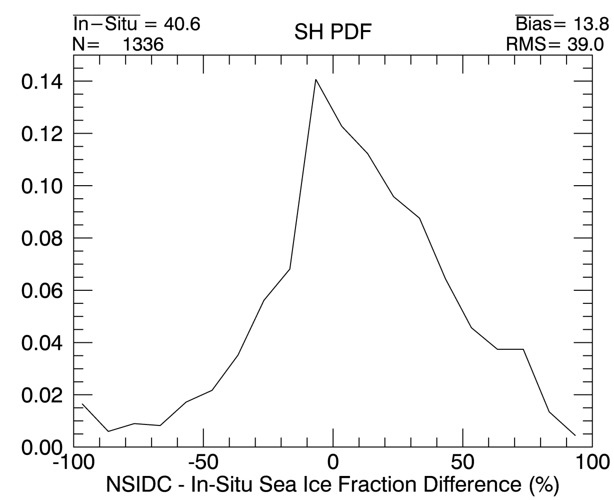

Sea ice fraction comparison between SSF and in-situ observations: clear and overcast

- For clear-sky, imager-based sea ice fraction is greater than in-situ by about 27%, and the microwave-based sea ice fraction is greater than in-situ by about 9%.

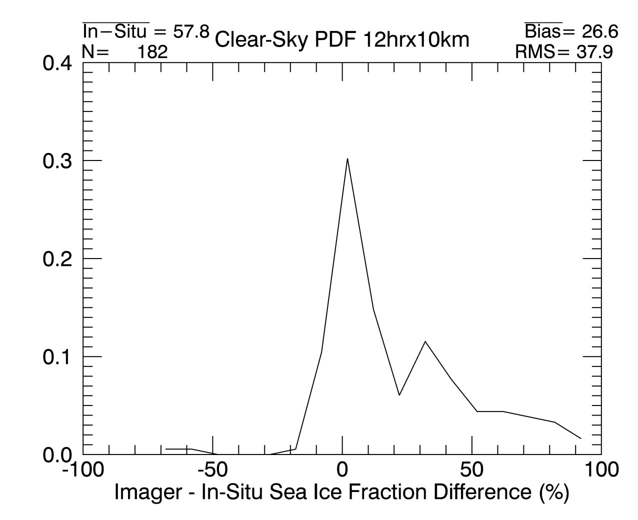

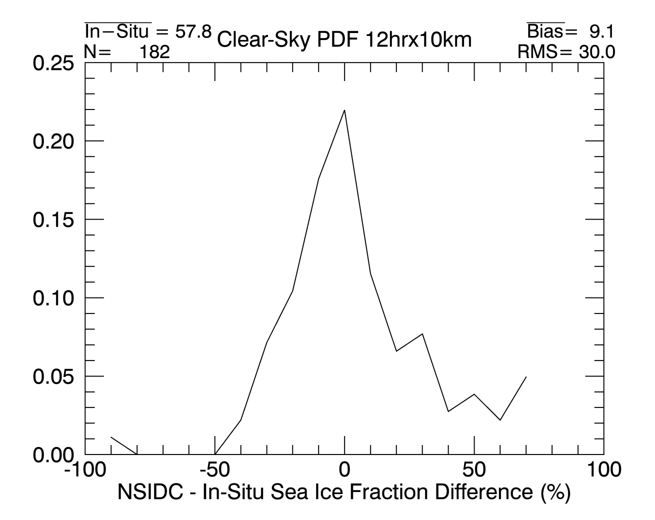

- For overcast conditions, the difference between microwave-based the the in-situ sea ice fraction is about 1.0%.

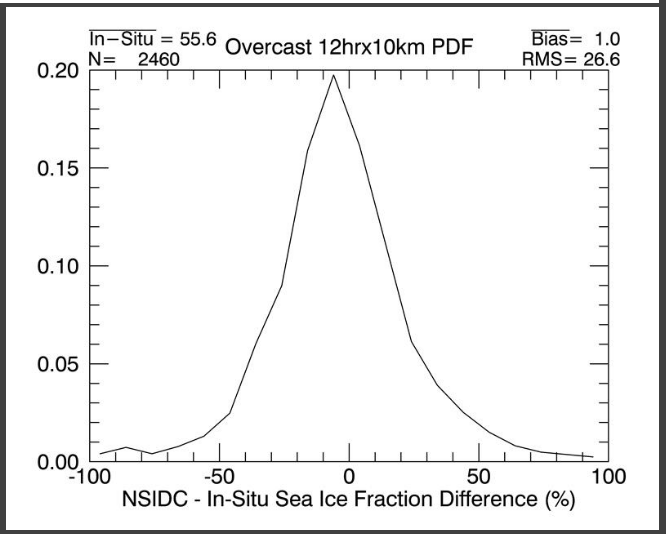

Microwave-based and imager-based sea ice fraction biases show no dependence on viewing zenith angles

VZA range (°)	Sample number	In-situ mean snow/ice fraction (%)	NSIDC		Imager-based	
			Mean bias (%)	Std dev (%)	Mean bias (%)	Std dev (%)
0-10	438	52.2	-0.7	36.6	35.7	51.0
10-20	505	57.1	-2.2	31.5	33.3	44.4
20-30	537	58.1	0.8	31.3	37.1	50.5
30-40	497	60.3	-0.4	29.5	33.2	44.9
40-50	541	59.7	2.6	32.1	33.0	46.1
50-60	441	59.1	0.5	30.6	36.5	49.2
60-70	347	59.3	0.4	28.7	37.3	50.5

CERES unfiltering algorithm

- Filters are placed in front of the radiometers to measure the energies from the SW, WN, and total portions of the spectrum.
- These filtered radiances are dependent upon how the radiation is filtered through the instrument optics.
- A procedure is applied that corrects for the spectral response of the instrument to produce "unfiltered" radiances that represent the radiation received by the instrument prior to entering the optics.
- This procedure also separates the radiance measurements into reflected solar and emitted thermal energy category.

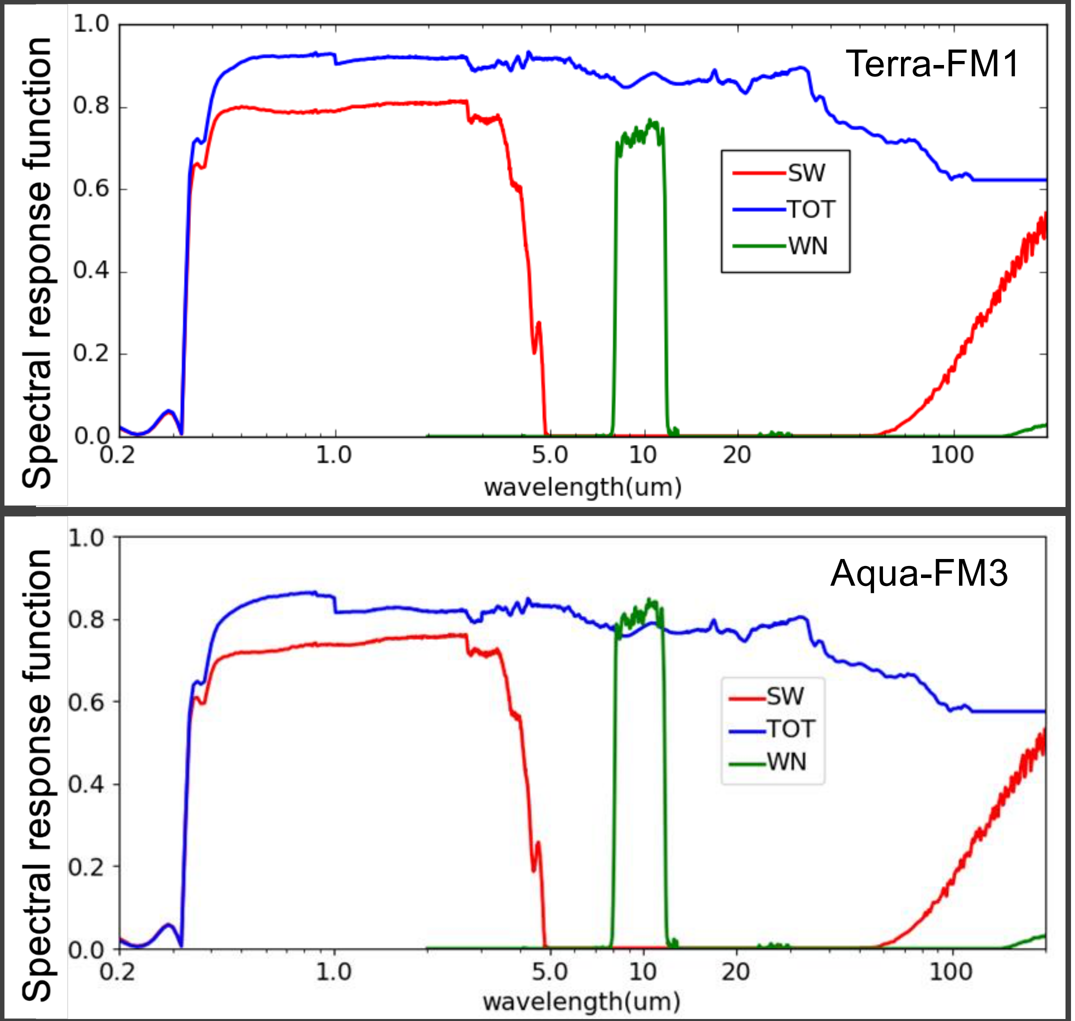

Deriving regression coefficients

- Calculate unfiltered reflected SW broadband radiances:

$$m_u^{SW\,r} = \int_0^\infty I_\lambda^r d\lambda$$

- Apply CERES spectral response functions to calculate the filtered reflected broadband radiances:

$$m_u^{SW\,r} = \int_0^\infty S_\lambda^{SW} I_\lambda^r d\lambda$$

- Derive the regression coefficients between unfiltered reflected SW radiance and filtered reflected SW radiances for every angular bin over typical Earth scenes:

$$m_u^{SW\,r} = a_0 + a_1 m_f^{SW\,r} + a_2 (m_f^{SW\,r})^2$$

MODTRAN simulation over clear ocean

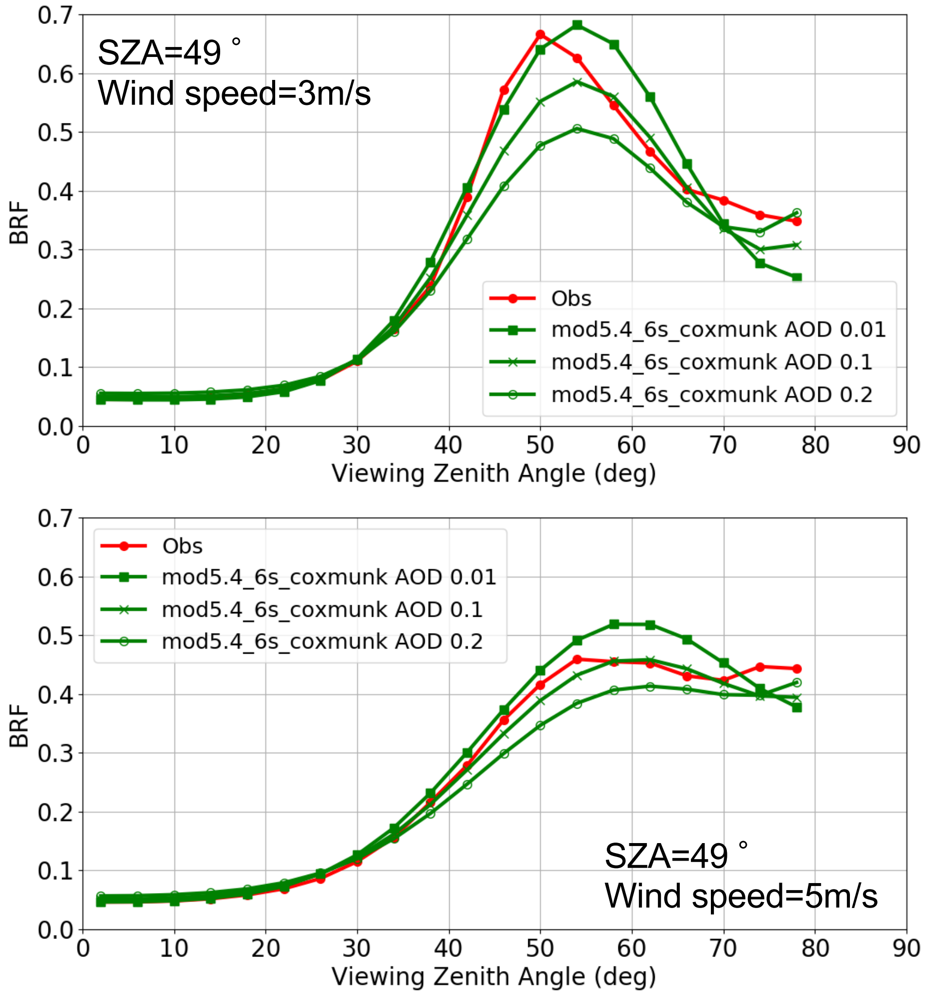

- Incorporated the CoxMunk BRDF model into the MODTRAN 5.4.
- Tropical profile, CoxMunk BRDF model with wind speed=5m/s
- Θ_0: 0, 29, 41.4, 51.3, 60, 68, 75.5, 80.3 and 85
- Θ: 0, 30, 45, 60 and 90
- Φ: 0, 7.5, 37.5, 90.0, 142.5, 172.5
- Maritime aerosol model with optical depths: 0, 0.055, 0.09, 0.16, 0.30, 0.67, 1.2
- Regression coefficients are calculated for each (Θ_0, Θ, Φ)
- Using solar spectrum irradiance with 0.025 nm resolution from Coddington et al. (2015)

The impact on clear ocean unfiltering is very small

- These regression coefficients are used to derive the CERES unfiltered radiances.
- Fluxes inverted from these radiances are compared with those in the CERES Edition 4 SSF data using the existing unfiltering algorithm.

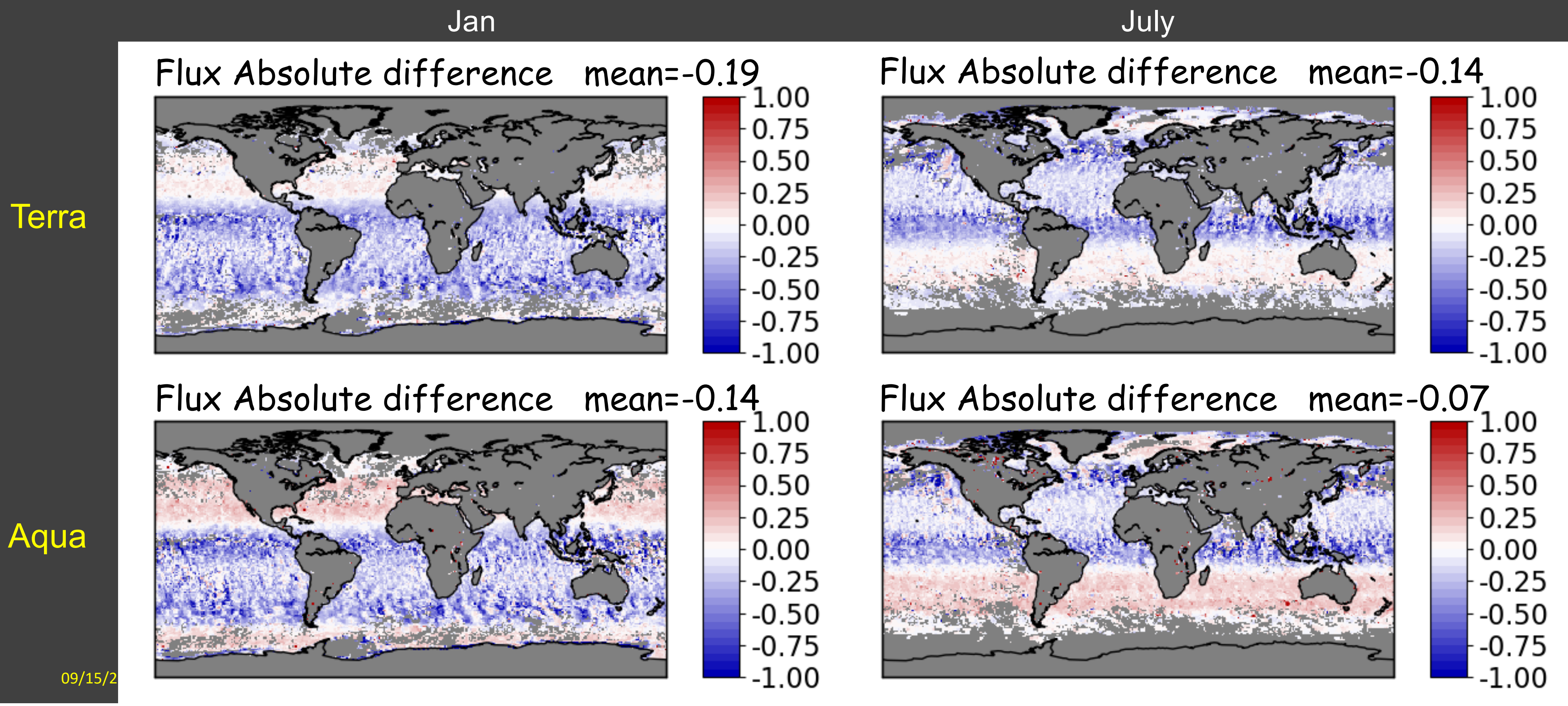

Wind speed has very small impact on clear ocean unfiltering algorithm

Flux difference using regressions derived with wind speed of 3 m/s and 5 m/s

Flux difference using regressions derived with wind speed of 7 m/s and 5 m/s

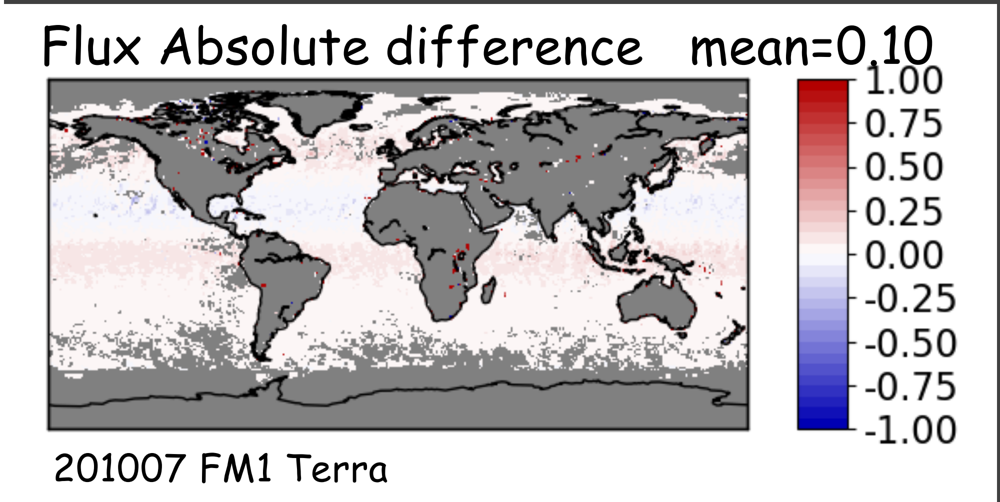

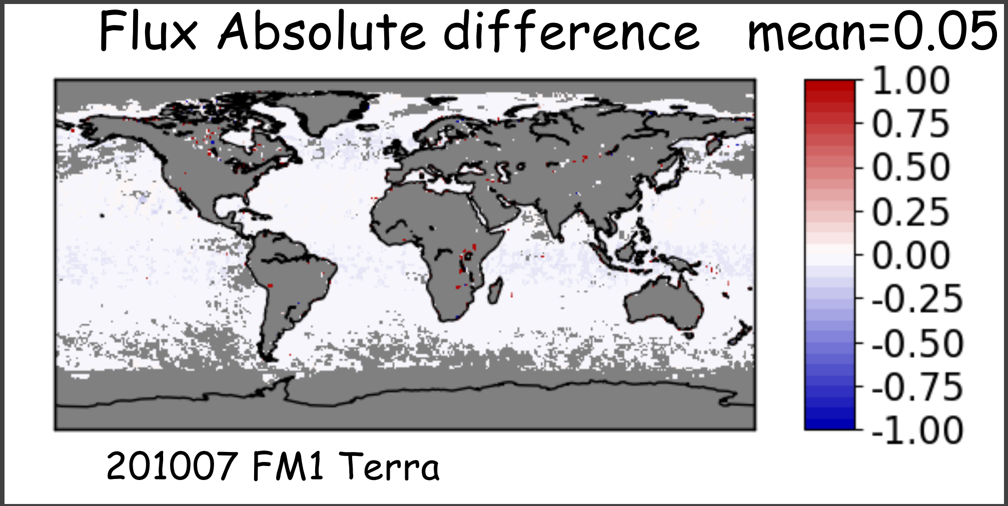

Unfiltering algorithm over clear ocean shows small sensitivity to aerosol type

- Flux difference using regressions derive with dust aerosols and maritime aerosols, both are with wind speed of 5 m/s
- Global mean difference is about 0.15 Wm-2, and difference at the grid box level is less than 1.0 Wm-2
- Using unfiltering coefficients developed from maritime aerosols for dust aerosols can lead to an overestimation of instantaneous flux up to 1.0 Wm-2.

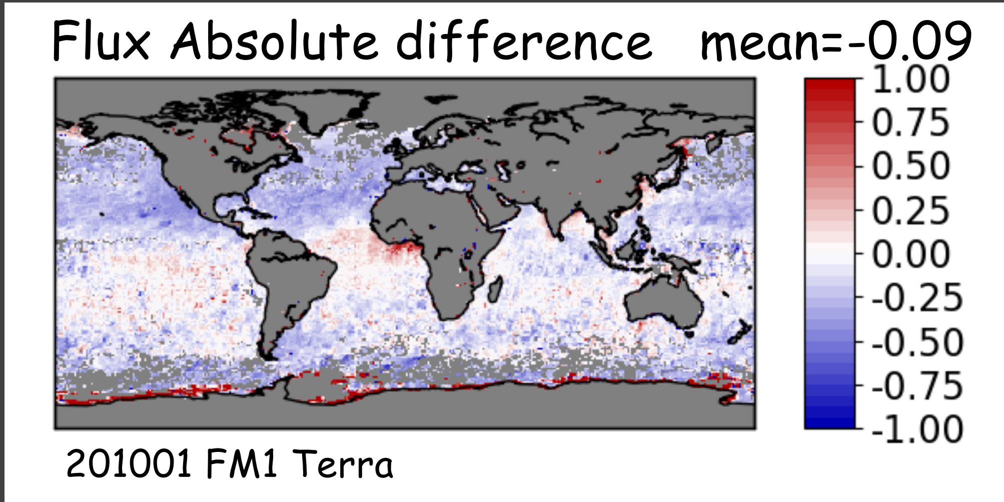

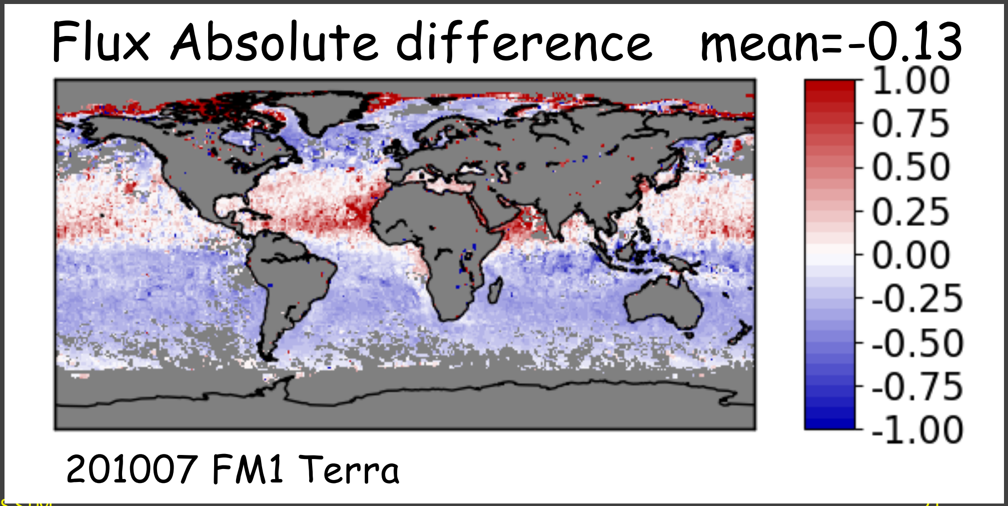

MODTRAN simulation over cloudy ocean

- Overcast clouds:
  - Ice clouds with optical depths of 4, 50
  - Stratus with optical depths of 5.6
  - Cumulus with optical depth of 217
- Mix with clear ocean simulations to construct partly cloudy cases with cloud fractions of 0.25, 0.50, 0.75
- Θ_0: 0, 29, 41.4, 51.3, 60, 68, 75.5, 80.3 and 85
- Θ: 0, 30, 45, 60 and 90
- Φ: 0, 7.5, 37.5, 90.0, 142.5, 172.5
- Regression coefficients are calculated for each (Θ_0, Θ, Φ)
- Using solar spectrum irradiance with 0.025 nm resolution from Coddington et al. (2015)

The impact on cloudy ocean unfiltering is very small (within 0.1%)

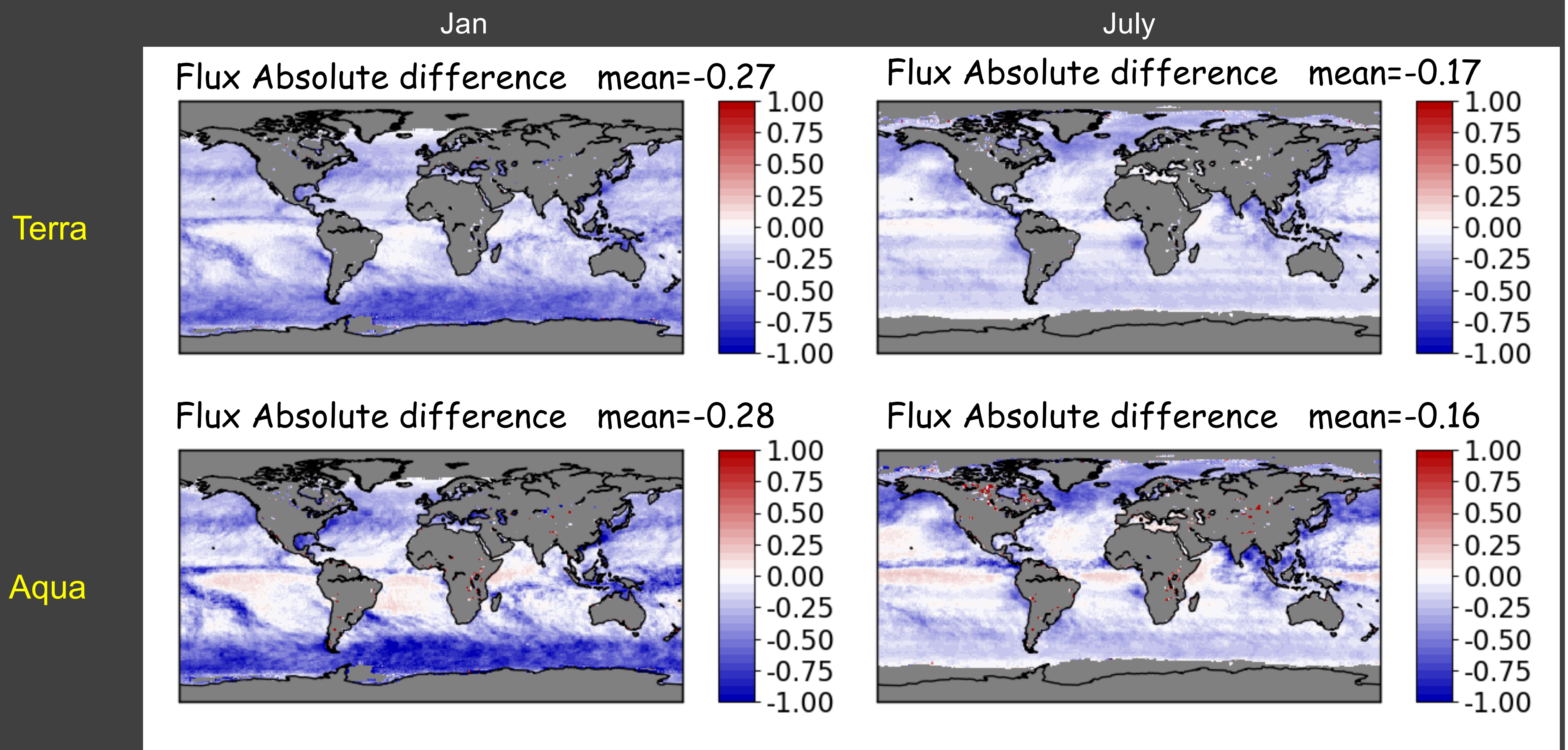

MODTRAN simulation over clear land

- Unfiltering coefficients are developed for the four seasons using RossLi model and 10-year mean of the kernel weights from MODIS
- Five surface types are considered, each paired with AODs and atmospheric profiles:
  - Forest
  - Savanna
  - Grassland and crops
  - Dark desert
  - Bright desert
- Θ_0: 0, 29, 41.4, 51.3, 60, 68, 75.5, 80.3 and 85
- Θ: 0, 30, 45, 60 and 90
- Φ: 0, 7.5, 37.5, 90.0, 142.5, 172.5
- Regression coefficients are calculated for each (Θ_0, Θ, Φ), each season, and each surface
- Using solar spectrum irradiance with 0.025 nm resolution from Coddington et al. (2015)

Flux difference between using the new vs. the old unfiltering coefficients: clear land

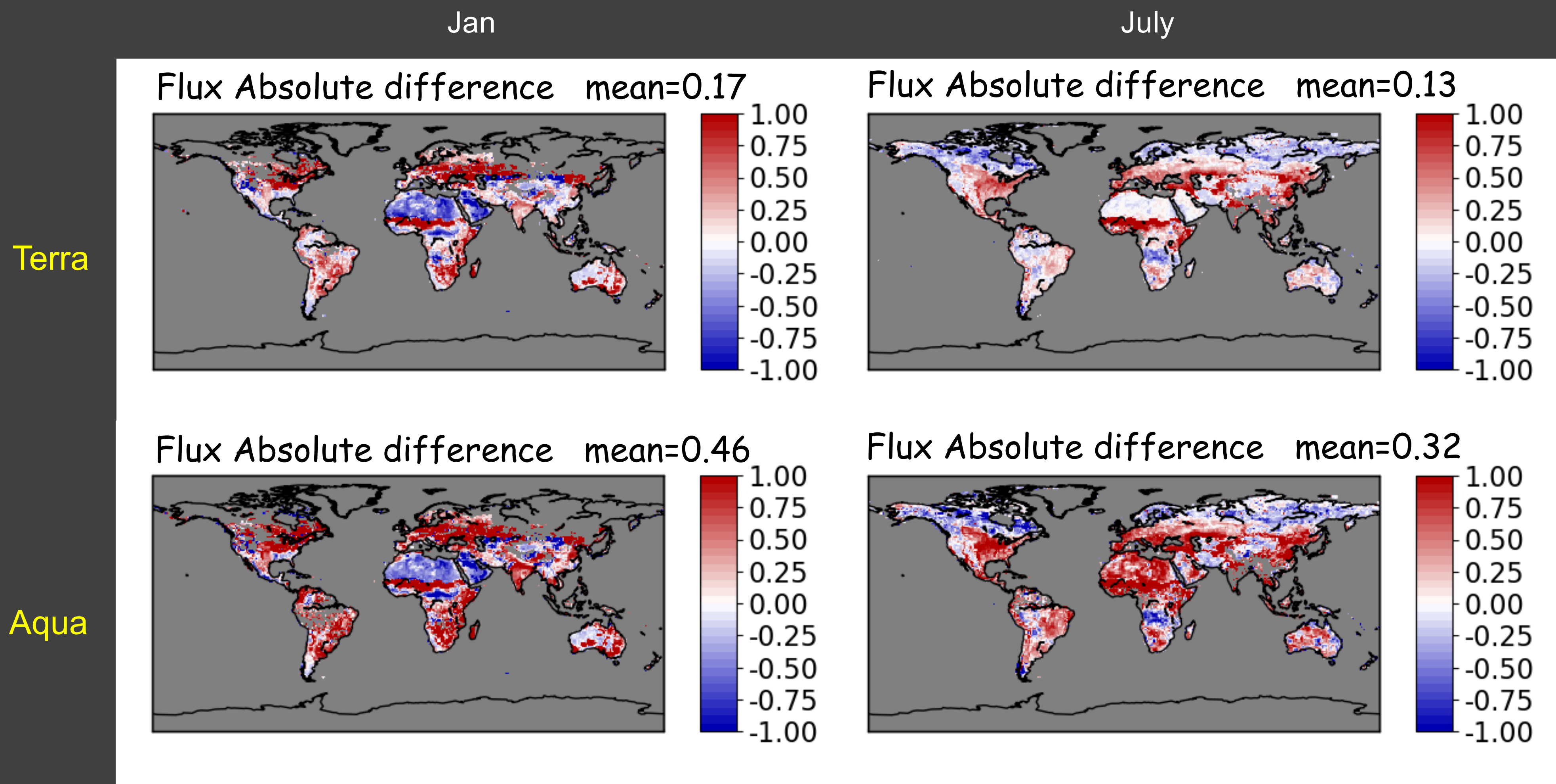

Sensitivity to seasonal coefficients

- Flux difference from using summer coefficients for winter, and winter coefficients for summer

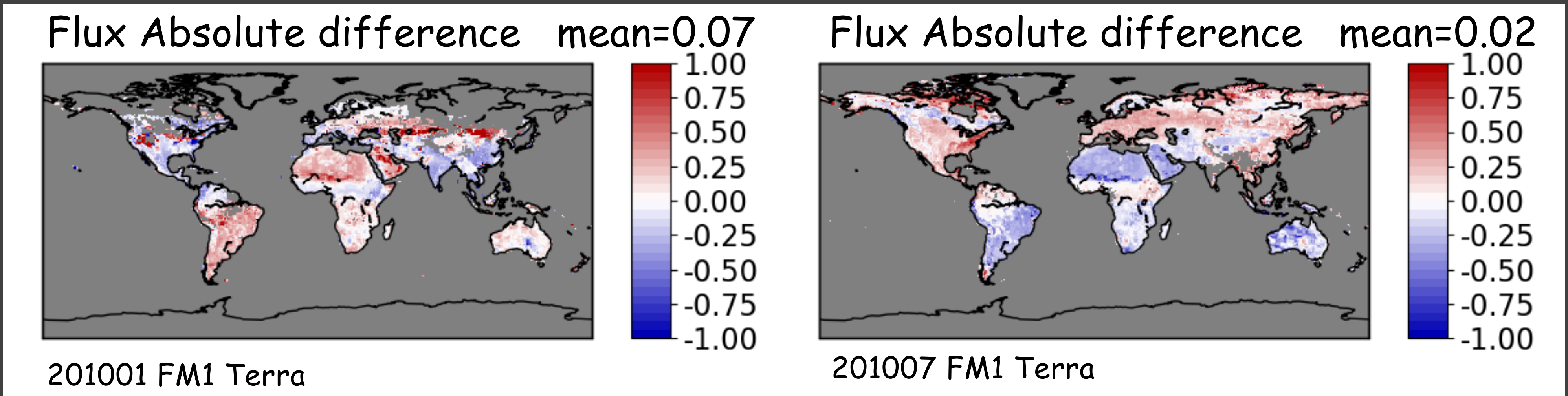

MODTRAN simulation over cloudy land

- Overcast clouds:
  - Ice clouds with optical depths of 4 and 50
  - Stratus with optical depths of 5.6
  - Cumulus with optical depth of 217
- Mix with clear land simulations to construct partly cloudy cases with cloud fractions of 0.25, 0.50, 0.75, and 1.0
- Θ_0: 0, 29, 41.4, 51.3, 60, 68, 75.5, 80.3 and 85
- Θ: 0, 30, 45, 60 and 90
- Φ: 0, 7.5, 37.5, 90.0, 142.5, 172.5
- Regression coefficients are calculated for each (Θ_0, Θ, Φ), each season, and each surface
- Using solar spectrum irradiance with 0.025 nm resolution from Coddington et al. (2015)

Flux difference between using the new vs. the old unfiltering coefficients: cloudy land

Jan July

Terra

Aqua

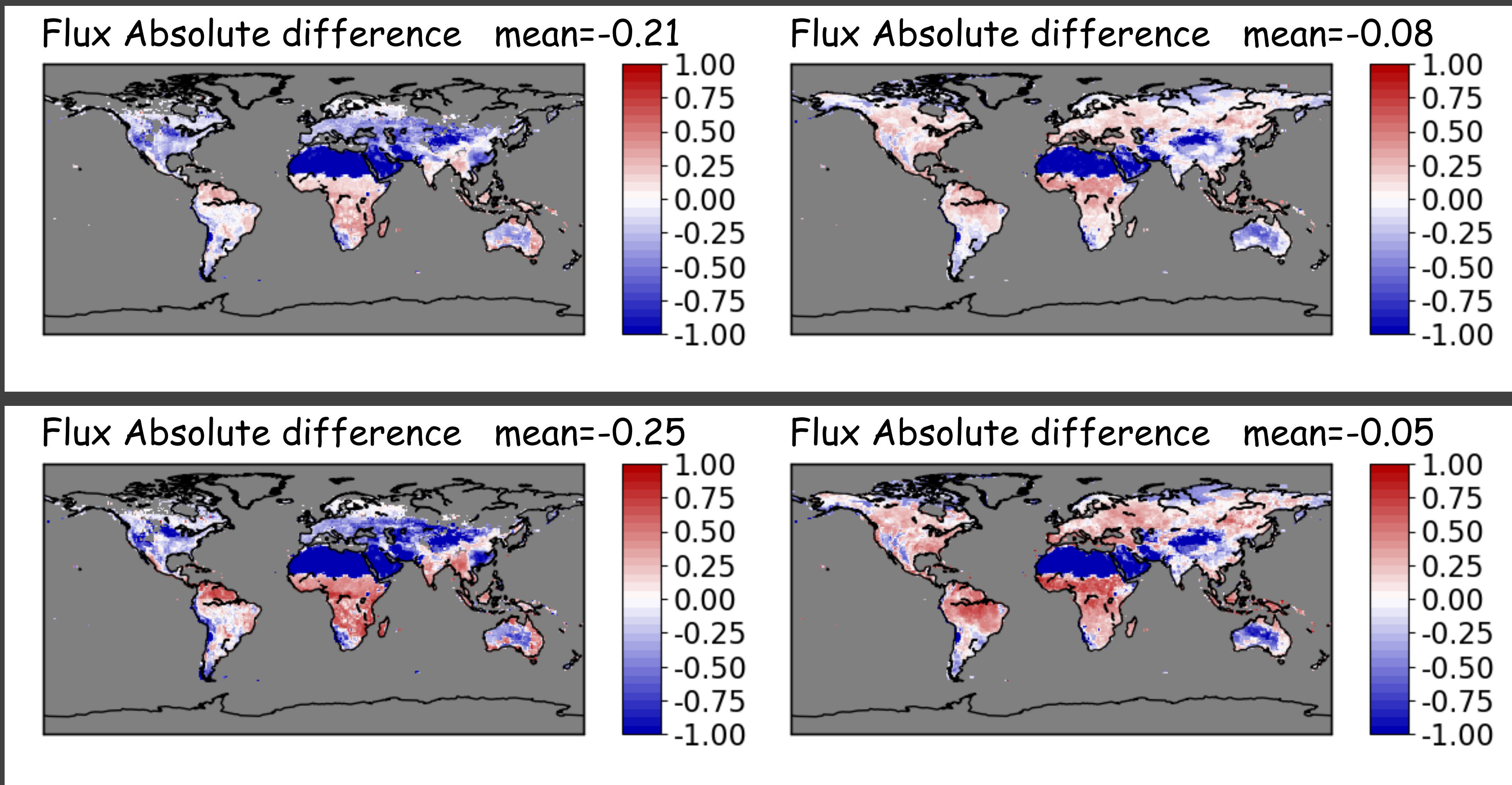

All-sky flux difference

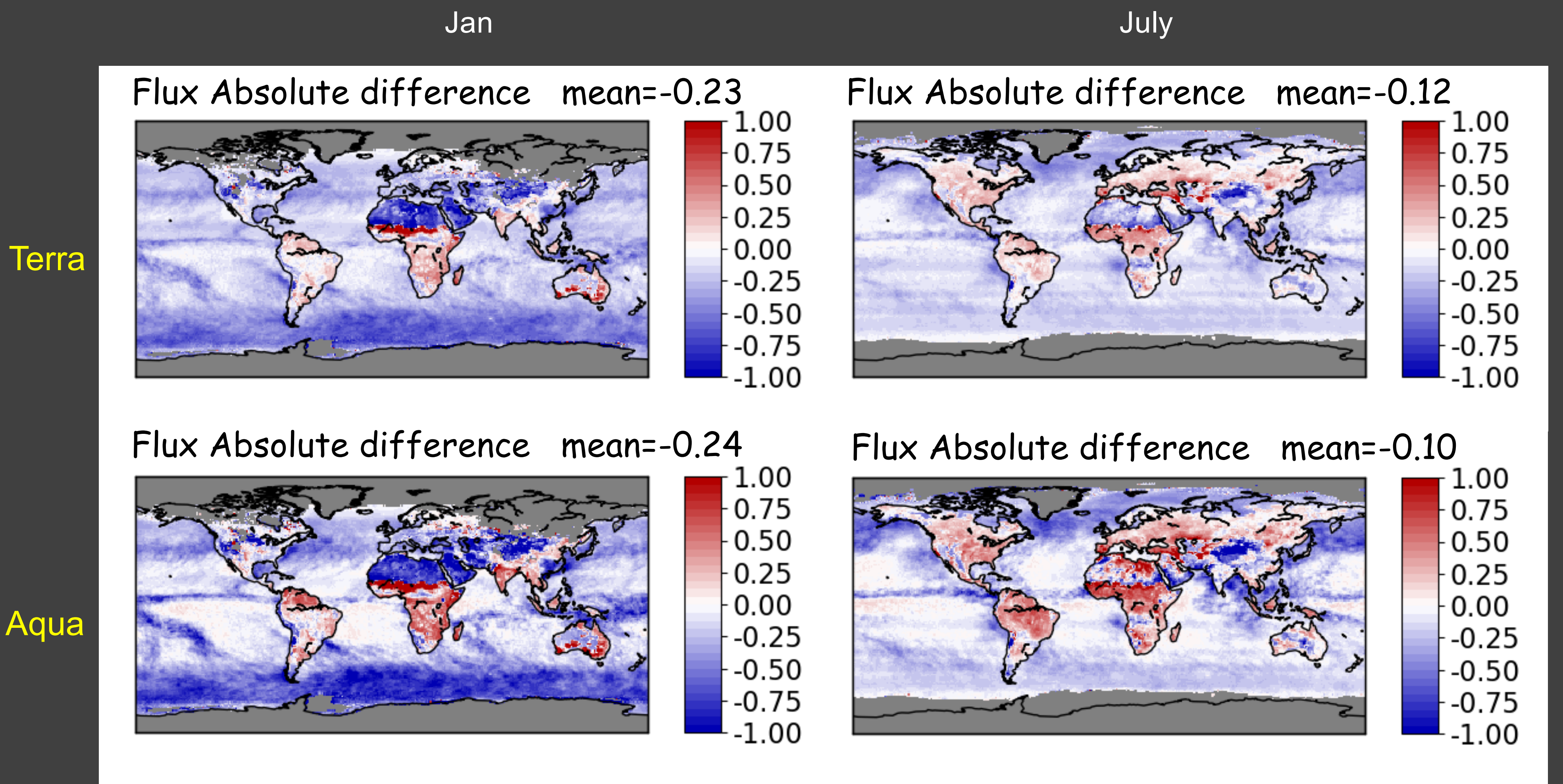

Radiance and flux inter-comparison between Terra and Aqua over the northern high latitude regions

- The descending node of the Terra orbit intersects with the ascending node of the Aqua orbit at 69°N, offering a unique opportunity to directly compare the near-simultaneous Terra and Aqua radiances/fluxes.
- Matching near-nadir (VZA<10°) footprints for flux/radiance comparisons:
  - Latitude/longitude differences < 0.1°
  - SZA and VZA differences < 2°, and RAZ difference < 5°
  - Consistent scene identifications
  - Overpass time difference < 1 hour → overpass time differences are all less than 20 minutes
- Focus on matched daytime footprints between 60-70° N hereafter using data from JJA 2018
- A total of ~24.7k matched footprints: 16k over land, 8.7k over ocean

LW radiance/flux difference between matched Terra and Aqua footprints

Radiance

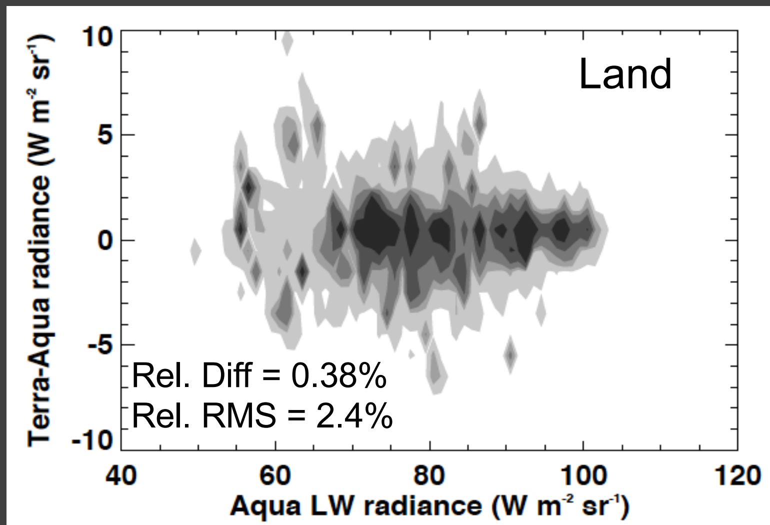

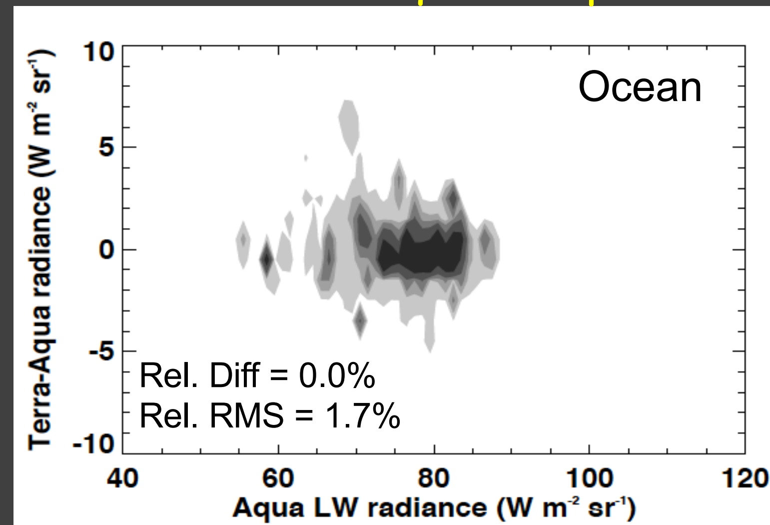

Flux

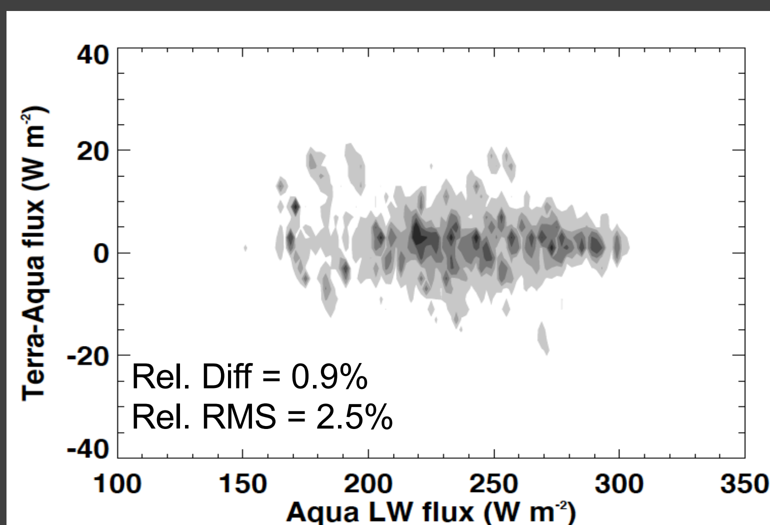

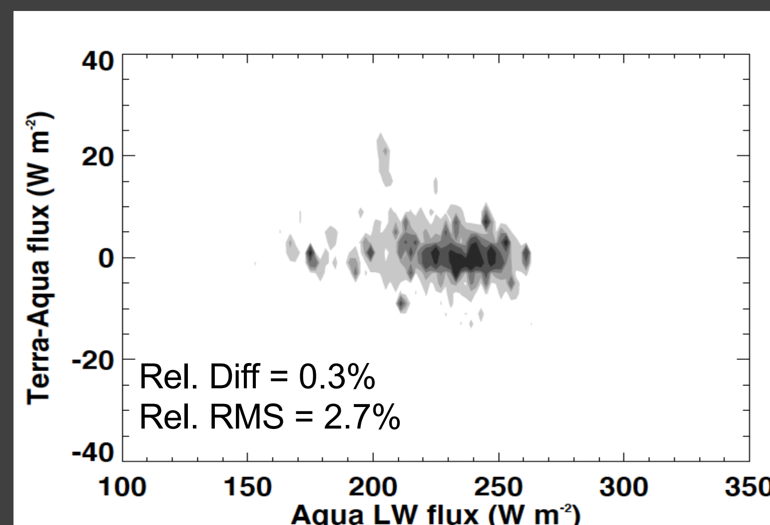

SW radiance/flux difference between matched Terra and Aqua footprints

Radiance

Flux

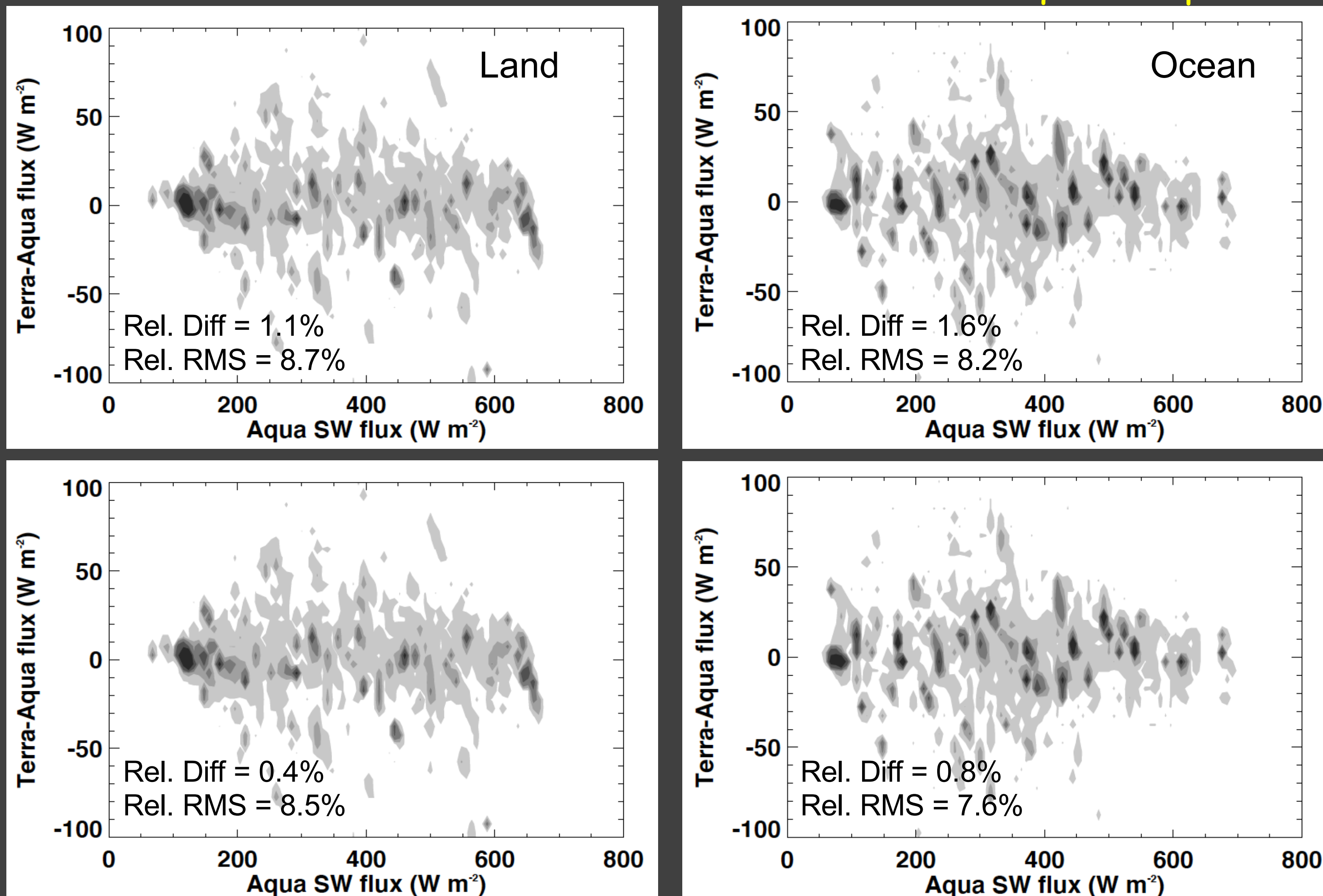

Cloud difference between matched Terra and Aqua footprints

Cloud fraction

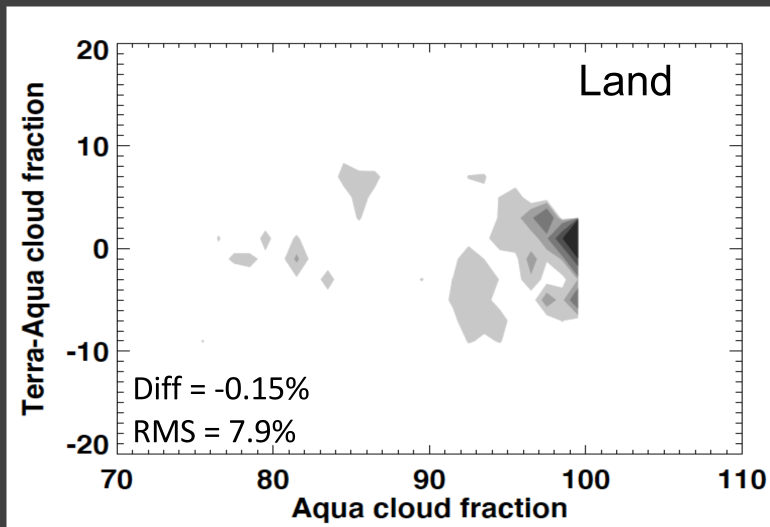

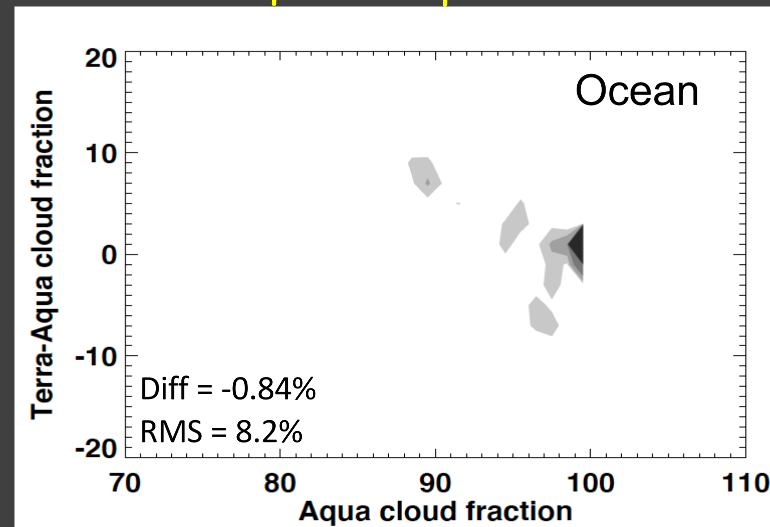

Cloud optical depth

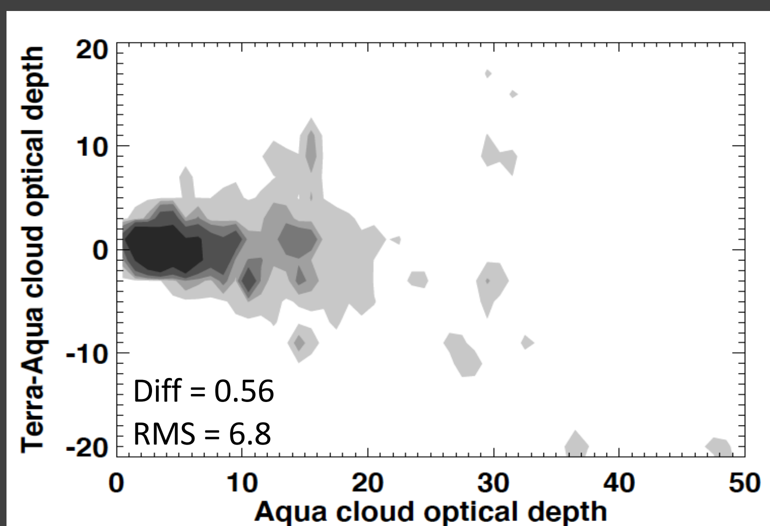

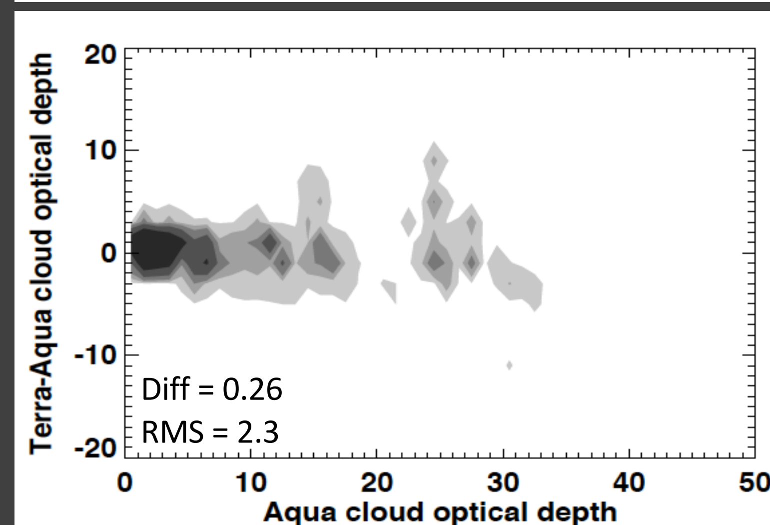

Summary

- CERES NPP is in RAPS mode since the end of March 2020. Initial check shows that the RAPS data look good.
- Imager-based snow/ice concentration is greater than the microwave-based snow/ice concentration.
- Comparison against in-situ sea ice observation indicates that the imager-based sea ice concentration is biased high, whereas the microwave-based sea ice concentration has a smaller bias.
- SW unfiltering algorithms impact the global monthly mean instantaneous SW flux by about 0.2 Wm-2. Regionally, SW flux difference can be up to 1 Wm-2.
- Collocated Terra and Aqua footprints over the northern high latitudes show that the SW radiances agree within 1.6%, and the daytime LW radiance agree within 0.4%.